Dufour and Soret Influence on MHD of an Oldroyd-B Fluid over a Stretching Sheet with Nanoparticles

Abdelmgid Osman Mohamed Sidahmed[1,*]

1   Department of Mathematics, College of Science & Arts, King Abdulaziz University, Rabigh 21911, Saudi Arabia

ARTICLE INFO	ABSTRACT
            	In this study, the heat and mass transfer characteristics of a two-dimensional incompressible Oldroyd-B fluid over a stretching sheet in the presence of Soret, Dufour, and nanoparticles are investigated. The effects of elasticity and magnetohydrodynamics on flow are being studied. The transport equations contain Brownian motion and thermophoresis. The governing partial differential equations and associated boundary conditions are dimension less using sufficient similarity variables. The resulting ordinary differential equations are solved using the successive linearization method. It has been quantitatively measured and explored how different embedded thermophysical characteristics affect fluid velocity, temperature, concentration, Nusselt number, and Sherwood number. The temperature and concentration distribution increase when the values of Du and Sr rise. As Nb estimations rise, Nusselt number estimates fall. It should be emphasized that the influence is shown to be quite modest as a retardation time is increased. A comparison of one instance of our findings with those previously published in the literature reveals a very strong agreement.

1. Introduction

The numerous industrial and engineering uses of non-Newtonian fluid analysis make it of utmost significance. These fluids are specifically used in the food industry, bioengineering, oil reservoir engineering, the chemical industry, and the nuclear industry. They are also used in the processing of materials. Many fluids, including paints, paper pulp, shampoos, ketchup, apple sauce, slurries, certain oils, and polymer solutions, do not obey Newton's laws of physics. There is no single constitutive connection that can account for all the non-Newtonian fluids' properties. For the properties of non-Newtonian fluids, several fluid models have been put forth in the literature. The three categories of differential type, rate type, and integral type are used to categorize non-Newtonian materials in general. The Maxwell fluid model represents the most straightforward class of rate-type fluids. The only aspects of relaxation time that are described by this model The Maxwell fluid is incapable of foretelling the properties of retardation time. Both the relaxation and retardation time characteristics were investigated using an Oldroyd-B fluid model (see references [1-4]). Shaqfeh [5] studied the flow

---

instabilities that occur when inertial forces are absent. An analysis of the numerical simulation of viscoelastic liquids based on molecular models was performed by Laso and Ottinger [6]. Sajid *et al.,* [7] started the boundary layer stagnation point flow toward a moving sheet in an Oldroyd-B model. For the distribution of velocities at infinite velocity, they provided numerical solutions. In the presence of Soret, Dufour, and nanoparticles, Venkatesh *et al.,* [8] investigated the heat and mass transfer characteristics of a two-dimensional incompressible electrically conducting Maxwell fluid over a stretching sheet. The numerical simulation of a three-dimensional Oldroyd-B fluid with time dependency by Motsa *et al.,* [9] was presented. By Hayat *et al.,* [10], in the context of the magnetohydrodynamic flow of an Oldroyd-B fluid, Cattaneo-Christov heat flux was examined in the presence of homogeneous and heterogeneous processes. Some recent investigations on Oldroyd-B fluids can be seen in the references [11-16].

Most cosmic events that we face daily in science, physics, and geometry may be modeled using nonlinear equations. Some of these nonlinear equations can be resolved using approximate mathematical analytical techniques, such as the Homotopy (HAM) analysis method developed by Liao [17] and the Adomain decomposition method (ADM) Makinde [18]. Traditional numerical methods like the Keller box, Runge-Kutta, and finite difference methods can be used to solve some of these equations. The successive linearization method (SLM), a technique, has been proven beneficial in recent studies. This method has been used to resolve many non-linear problems in science and engineering. The governing non-linear equations have been transformed into a system of linear differential equations using this method. We applied the Chebyshev pseudo-spectral method to solve the higher-order deformation in linear differential equations. As an alternative to more conventional numerical methods, the SLM methodology can be utilized to solve boundary value issues involving highly non-linear systems (see references [19-26]).

The driving potentials are more complicated and difficult to comprehend when both heat and mass transport take place at the same time. Composition gradients result in the Dufour effect, which describes the movement of energy that this gradient causes. The Soret effect, also called the thermal-diffusion effect, is the ability of temperature gradients to cause mass flows. It can be seen in mixtures of fluids and particles that are suspended in the air. These phenomena are caused by the transfer of nanoparticles into the cold zone, which is triggered by the mobility of fluid molecules and high energy levels in the hot zone. Because of the size of the fluid molecules and the particle, this force is only significant at low fluid velocities, such as in natural convection. The Soret number increases the velocity and concentration profiles, according to Venkateswarlu and Satya [27] analysis of the effects of Soret and Dufour on the MHD stream of a Maxwell fluid on a stretched surface using joule heating. According to Hayat *et al.,* [28] analysis of Soret and Dufour's effects on the MHD stream of Casson fluid, velocity decreases as the Casson parameter rises. Khan *et al.,* [29] studded the simultaneous features of soret and dufour in entropy optimized flow of reiner-rivlin fluid considering thermal radiation. There has been some recent research in this area, including the many impacts mentioned in References [30-32].

The thermal conductivity of nanofluids is higher than that of non-nanofluids. Since solids transfer heat more efficiently than liquids, a fluid's thermal conductivity can be increased by suspending solid particles like metals (gold, silver), carbon (nanotubes), and silicon in the fluid. Base fluids are frequently aqueous solutions like crude oil, liquid hydrocarbons, etc. [33]. As revealed by Gholinia *et al.,* [34], the form of the nanoparticles has a significant impact on the heat transfer rate. For instance, cylinder-shaped nanoparticles exhibit stronger thermal conductivity than brick-shaped ones, but they do so at a slower pace than lamina-shaped ones. Doh *et al.,* [35] have conducted research on the impact of magnetic nanofluids on thermal conductivity. They stated that the heat conductivity is

significantly increased (by more than 100%) as a result of the magnetic field these nanoparticles produce. Further studies in this direction are mentioned in references [36-42].

The studies mentioned above revealed that no research on the heat and mass transfer characteristics of a two-dimensional incompressible Oldroyd-B fluid over a stretching sheet in the presence of Soret, Dufour, and nanoparticles has been done. This investigation aims to describe the heat and mass transfer properties of an Oldroyd-B fluid that streams across a stretched sheet in the presence of Soret, Dufour, and nanoparticles in an incompressible, two-dimensional steady state. The problem raised here is a fundamental one that manifests itself in numerous real-world contexts, including the polymer extrusion procedure. The Soret effect has been used to create low molecular weight gas mixtures for isotope separation. The reduced ordinary differential equations are resolved using the successive linearization technique. When compared to those presently available, current results are in excellent agreement with data that was previously available.

2. Mathematical Formulation
2.1 Governing Equations and Boundary Conditions

Consider a steady, incompressible two-dimensional fluid that is flowing through a stretched sheet. MHD and nanoparticle effects are saturated as the sheet expands with the plane $Y = 0$. It is assumed that the flow is constrained to $Y > 0$. We should posit the possibility that the sheet is stretched continuously with $U(X) = aX$, where $a > 0$ is constant and the $x-$axis is approximated along the stretching surface. The stretched surface is given a magnetic field that is consistently consistent and uniform in a normal direction. Figure 1 shows that the induced magnetic field has very little impact. Under the constant and boundary layer assumptions, the continuous constitutive equation of the Oldroyd-B fluid and energy equation is presented below as reference [8] and [43].
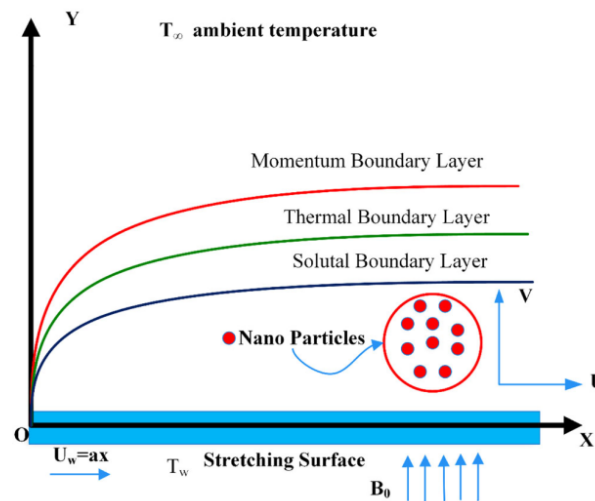

Fig. 1. Physical configuration of the model

$$\frac{\partial U}{\partial X} + \frac{\partial V}{\partial Y} = 0, \tag{1}$$

$$U\frac{\partial U}{\partial X} + V\frac{\partial U}{\partial Y} + \beta\left(U^2\frac{\partial^2 U}{\partial X^2} + V^2\frac{\partial^2 U}{\partial Y^2} + 2UV\frac{\partial^2 U}{\partial X\partial Y}\right) = v\left[\frac{\partial^2 U}{\partial Y^2} + \gamma\left(\frac{\partial}{\partial X}\left(U\frac{\partial^2 U}{\partial Y^2}\right) + \frac{\partial U}{\partial Y}\frac{\partial^2 V}{\partial Y^2} + V\frac{\partial^3 U}{\partial Y^3}\right)\right] - \frac{\sigma B_0^2}{\rho}\left(U + \beta V\frac{\partial U}{\partial Y}\right), \tag{2}$$

$$U\frac{\partial T}{\partial X} + V\frac{\partial T}{\partial Y} = \alpha\left(\frac{\partial^2 T}{\partial X^2} + \frac{\partial^2 T}{\partial Y^2}\right) + \tau\left\{D_B\left(\frac{\partial C}{\partial X}\frac{\partial T}{\partial X} + \frac{\partial C}{\partial Y}\frac{\partial T}{\partial Y}\right) + \left(\frac{D_T}{T_\infty}\right)\left[\left(\frac{\partial T}{\partial X}\right)^2 + \left(\frac{\partial T}{\partial Y}\right)^2\right]\right\} + \frac{D_m K_T}{C_s C_P}\frac{\partial^2 C}{\partial Y^2}, \tag{3}$$

$$U \frac{\partial C}{\partial X} + V \frac{\partial C}{\partial Y} = D_B \left(\frac{\partial^2 C}{\partial X^2} + \frac{\partial^2 C}{\partial Y^2} \right) + \left(\frac{D_T}{T_\infty} \right) \left[\frac{\partial^2 T}{\partial X^2} + \frac{\partial^2 T}{\partial Y^2} \right] + \frac{D_m K_T}{T_m} \frac{\partial^2 T}{\partial Y^2}. \tag{4}$$

The corresponding boundary conditions are

$$U = U_w(x) = aX, \quad V = 0, \quad T = T_w, \quad C = C_w, \quad \text{at } Y = 0,$$
$$U = 0, \quad T = T_\infty, \quad V = 0, \quad C = C_\infty, \quad \text{as } Y \to \infty, \tag{5}$$

where (U, V) are the components of velocity in (X, Y) directions, The parameters $\beta, \upsilon \left(= \frac{\mu}{\rho} \right), \mu, \gamma, \rho, \sigma, B_0$ stand for the relaxation time, the kinematic viscosity, the dynamic viscosity, the retardation time, density of fluid, the electric conductivity and the uniform magnetic fluid respectively, α is the thermal diffusivity, T is the fluid temperature, C the nanoparticle fraction, T_w and C_w are the temperature of fluid and nanoparticle fraction at the wall, respectively, D_B is the Brownian diffusion D_T coefficient, is the thermophoretic diffusion coefficient, $\tau = \frac{(\rho C)_P}{(\rho C)_f}$ is the ratio between the effective heat capacity of the nanoparticle material and heat capacity of the fluid, C is the volumetric volume expansion coefficient and ρ_P is the density of the particles.

2.2 Similarity Transformation

The following non-dimensional variables [8, 43-45] can be used to convert the governing Eq. (2)-(4) into a set of nonlinear ordinary differential equations:

$$U = cXf'(\eta), V = -\sqrt{c\upsilon} f(\eta), \eta = \sqrt{\frac{c}{\upsilon}}, \theta = \frac{T - T_\infty}{T_w - T_\infty}, \phi = \frac{C - C_\infty}{C_w - C_\infty}. \tag{6}$$

The following set of non-linear ordinary differential equations is produced by applying Eq. (12) to the governing equations.

$$f''' + (1 + M\beta_1) ff'' - f'^2 + \beta_1 (2ff'f'' - f^2 f''') + \beta_2 \left(2f'f''' - f''^2 - ff^{iv} \right) - M^2 f' = 0, \tag{7}$$
$$\theta'' + Pr[f\theta' + Nb(\phi'\theta') + Nt(\theta')^2] + Pr\,(Du)\phi'' = 0, \tag{8}$$
$$\phi'' + Pr(Le)\,(f\phi') + \frac{Nt}{Nb}\theta'' + Sr\theta'' = 0. \tag{9}$$

Where

$\beta_1 (= \beta c)$ is the elastic parameter, $\beta_2 (= \gamma c)$ is Deborah number in terms of retardation time, $M^2 (= \sigma\beta_0^2 / c\rho)$ is the Hartman number, $Pr = \upsilon/\alpha$ is the Prandtl number, Nb the Brownian motion, Nt is the thermophoresis parameter, $Le = \alpha/D_B$ and is the Lewis number, Du is Dufour number, and Sr is Soret number.

The boundary conditions are:

$$f(0) = 0, \quad f'(0) = 1, \quad f'(\infty) = 0, \tag{10}$$
$$\theta(0) = 1, \quad \theta(\infty) = 1, \tag{11}$$
$$\phi(0) = 1, \quad \phi(\infty) = 0. \tag{12}$$

Expressions for C_f, Nu, and Sh are shown as follows:

$$C_f = \frac{\tau_w}{\rho u_e^2(x)} \ , \quad NU = \frac{Xq_w}{\alpha(T_w - T_\infty)} \ , Sh = \frac{Xq_m}{\alpha(C_w - C_\infty)} \tag{13}$$

Where q_w and q_m stand for the heat flux and mass flux, respectively, and w stands for the wall's shear stress:

$$\tau_w = \mu(1 + \beta_1)\left(\frac{\partial U}{\partial Y}\right)_{Y=0}, q_w = -\alpha\left(\frac{\partial T}{\partial Y}\right)_{Y=0}, q_m = -D_B\left(\frac{\partial C}{\partial Y}\right)_{Y=0}, \ Sr = \frac{D_M K_T(T_w - T_\infty)}{T_M(C_w - C_\infty)}\frac{1}{D_B}, \ Du = \frac{D_M K_T(C_w - C_\infty)}{T_M(T_w - T_\infty)}\frac{1}{D_B}. \tag{14}$$

The dimensionless formulation of Eq. (13) is [8]:

$$Re_x^{1/2}C_f = (1 + \beta_1)f''(0), Re_x^{1/2}Nu = -\theta'(0), \ Re_x^{(-1/2)}Sh = -\phi'(0), \tag{15}$$

Where $R_e(x) = u_w(x)x/v$ is the Reynolds number relative to the shrinking velocity $u_w(x)$.

3. Numerical Methods

We employ the successive linearization method to numerically solve the current problem. The SLM works by iteratively converting the controlling nonlinear Eq. (7) - (9) into a set of linear differential equations, which are then solved analytically or numerically.
The SLM technique presupposes that the solution of system Eq. (7)-(9) can be represented as [46-49]

$$f(\eta) = f_i(\eta) + \sum_{n=0}^{i-1} f_n(\eta), \quad \theta(\eta) = \theta_i(\eta) + \sum_{n=0}^{i-1} \theta_n(\eta), \quad \phi(\eta) = \phi_i(\eta) + \sum_{n=0}^{i-1} \phi_n(\eta) \tag{16}$$

Starting from an initial guess that is appropriate for $f_0(\eta)$, $\theta_0(\eta)$ and $\phi_0(\eta)$ and satisfies the boundary conditions as Eq. (10), Eq. (11) and Eq. (12), suitable functions are as follows.

$$f_0(\eta) = 1 - e^{-\eta}, \ \theta_0(\eta) = e^{-\eta}, \ \phi_0(\eta) = e^{-\eta} \tag{17}$$

Substituting Eq. (16) into the controlling Eq. (7)-(9) while neglecting the nonlinear factors in $f_i(\eta)$, $\theta_i(\eta)$ and $\phi_i(\eta)$ and their derivatives yields:

$$\left(-\beta_2 \sum_{j=0}^{i-1} f_j\right)f_i^{iv} + \left(1 - \beta_1\left(\sum_{j=0}^{i-1} f_j\right)^2 + 2\beta_2 \sum_{j=0}^{i-1} f_j'\right)f_i''' + \left((1 + M\beta_1)\sum_{j=0}^{i-1} f_j + 2\beta_1 \sum_{j=0}^{i-1} f_j \sum_{j=0}^{i-1} f_j'\right)f_i'' + \left(2\beta_1 \sum_{j=0}^{i-1} f_j \sum_{j=0}^{i-1} f_j'' - 2\sum_{j=0}^{i-1} f_j' + 2\beta_2 \sum_{j=0}^{i-1} f_j''' - M^2\right)f_i' + \left((1 + M\beta_1)\sum_{j=0}^{i-1} f_j'' + 2\beta_1 \sum_{j=0}^{i-1} f_j' \sum_{j=0}^{i-1} f_j'' - 2\beta_1 \sum_{j=0}^{i-1} f_j \sum_{j=0}^{i-1} f_j''' - \beta_2 \sum_{j=0}^{i-1} f_j^{iv}\right)f_i = r_{1,i-1} \tag{18}$$

$$\theta_i'' + Pr\left(\sum_{j=0}^{i-1} f_j + Nb \sum_{j=0}^{i-1} \phi_j' + 2Nt \sum_{j=0}^{i-1} \theta_j'\right)\theta_i' + \left(Pr \sum_{j=0}^{i-1} \theta_j'\right)f_i + Pr(Du)\phi_i'' + PrNb \sum_{j=0}^{i-1} \theta_j' \phi_i' = r_{2,i-1} \tag{19}$$

$$\phi_i'' + \left(Le\,Pr \sum_{j=0}^{i-1} f_j\right)\phi_i' + \left(Le\,Pr \sum_{j=0}^{i-1} \phi_j'\right)f_i + \left(\frac{Nt}{Nb} + Sr\right)\theta_i'' = r_{3,i-1} \tag{20}$$

Depending on the conditions at the boundary,

$$f_i(0) = f_i'(0) = f_i'(\infty) = 0, \theta_i(0) = \theta_i(\infty) = 0,$$
$$\phi_i(0) = \phi_i(\infty) = 0.$$

Where,

$$r_{1,i-1} = \beta_2 \sum_{j=0}^{i-1} f_j \sum_{j=0}^{i-1} f_j^{iv} - \sum_{j=0}^{i-1} f_j''' - (1 + M\beta_1) \sum_{j=0}^{i-1} f_j \sum_{j=0}^{i-1} f_j'' + \beta_1 \sum_{j=0}^{i-1} f_j''' \left(\sum_{j=0}^{i-1} f_j\right)^2 - 2\beta_1 \sum_{j=0}^{i-1} f_j \sum_{j=0}^{i-1} f_j' \sum_{j=0}^{i-1} f_j'' - 2\beta_2 \sum_{j=0}^{i-1} f_j \sum_{j=0}^{i-1} f_j''' + \beta_2 \left(\sum_{j=0}^{i-1} f_j''\right)^2 + \left(\sum_{j=0}^{i-1} f_j'\right)^2 + (\lambda + M) \sum_{j=0}^{i-1} f_j',$$

$$r_{2,i-1} = -\sum_{j=0}^{i-1} \theta_j'' - Pr \sum_{j=0}^{i-1} f_j \sum_{j=0}^{i-1} \theta_j' - Pr\, Nb \sum_{j=0}^{i-1} \phi'_j \sum_{j=0}^{i-1} \theta_j' - Pr\, Nt \left(\sum_{j=0}^{i-1} \theta'\right)^2 - (Pr)(Du) \sum_{j=0}^{i-1} \theta_j'',$$

$$r_{3,i-1} = -\sum_{j=0}^{i-1} \phi_j'' - Le\, Pr \sum_{j=0}^{i-1} f_j \sum_{j=0}^{i-1} \phi_j' - \frac{Nt}{Nb} \sum_{j=0}^{i-1} \theta_j'' - Sr \sum_{j=0}^{i-1} \theta_j'',$$

Using the Chebyshev collocation spectral method [50], the linearized system is solved, producing the following system of equations:

$$
\begin{aligned}
A_{11}\, f_i + A_{12}\, \theta_i + A_{13}\, \phi_i &= r_{1,i-1} \\
A_{21}\, f_i + A_{22}\, \theta_i + A_{23}\, \phi_i &= r_{2,i-1} \\
A_{31}\, f_i + A_{32}\, \theta_i + A_{33}\, \phi_i &= r_{3,i-1}
\end{aligned}
\tag{21}
$$

We can write system Eq. (21) as matrix equation as
$$A_{i-1} X_i = R_{i-1}, \tag{22}$$

Where,

$$A_{i-1} = \begin{bmatrix} A_{11} & A_{12} & A_{13} \\ A_{21} & A_{22} & A_{23} \\ A_{31} & A_{32} & A_{33} \end{bmatrix}, \ X_i = \begin{bmatrix} f_i \\ \theta_i \\ \phi_i \end{bmatrix}, \ R_{i-1} = \begin{bmatrix} r_{1,i-1} \\ r_{2,i-1} \\ r_{3,i-1} \end{bmatrix},$$

And

$$A_{11} = \left(-\beta_2 \sum_{j=0}^{i-1} f_j\right)D^4 + \left(1 - \beta_1 \left(\sum_{j=0}^{i-1} f_j\right)^2 + 2\beta_2 \sum_{j=0}^{i-1} f_j'\right)D^3 + \left((1+M\beta_1) \sum_{j=0}^{i-1} f_j + 2\beta_1 \sum_{j=0}^{i-1} f_j \sum_{j=0}^{i-1} f_j'\right)D^2 + \left(2\beta_1 \sum_{j=0}^{i-1} f_j \sum_{j=0}^{i-1} f_j'' - 2 \sum_{j=0}^{i-1} f_j' + 2\beta_2 \sum_{j=0}^{i-1} f_j''' - M^2\right)D + \left((1+M\beta_1) \sum_{j=0}^{i-1} f_j'' + 2\beta_1 \sum_{j=0}^{i-1} f_j' \sum_{j=0}^{i-1} f_j'' - 2\beta_1 \sum_{j=0}^{i-1} f_j \sum_{j=0}^{i-1} f_j''' - \beta_2 \sum_{j=0}^{i-1} f_j^{iv}\right),$$

$$A_{12} = A_{13} = 0, A_{21} = \left(Pr \sum_{j=0}^{i-1} \theta_j'\right),$$

$$A_{22} = D^2 + Pr\left(\sum_{j=0}^{i-1} f_j + Nb \sum_{j=0}^{i-1} \phi_j' + 2Nt \sum_{j=0}^{i-1} \theta_j'\right)D,$$

$$A_{23} = Pr(Du)\, D^2 + \left(PrNb \sum_{j=0}^{i-1} \theta_j'\right)D, A_{31} = \left(Le\, Pr \sum_{j=0}^{i-1} \phi_j'\right),$$

$$A_{32} \left(\frac{Nt}{Nb} + Sr\right) D^2, A_{33} = D^2 + \left(Le\, Pr \sum_{j=0}^{i-1} f_j\right)D.$$

The resultant system Eq. (22) is readily solved as

$$\boldsymbol{X} = A_{i-1}^{-1} R_{i-1} \tag{23}$$

4. Convergence Analysis

The convergence of series solutions to the momentum, temperature, and concentration equations is shown in Table 1. It should be observed that the convergence of $f''(0)$ requires a 4th-order approximation, while $\theta'(0)$ requires a 12th-order approximation, and $\phi'(0)$ requires a 13th-order approximation.

Table 1
Convergence of SLM solutions with respect to several orders of approximations when $Pr = 10, Le = M = 1, Sr = Nb = Nt = \beta_1 = 0.1, Du = \beta_2 = 0.01$

Order of approximation	$-f''(0)$	$-\theta'(0)$	$-\phi'(0)$
1	1.427526290	0.937804159	1.808246528
3	1.438897811	0.937266679	1.920490523
4	1.438897811	0.936859200	1.920969679
10	1.438897811	0.936947042	1.920870392
12	1.438897811	0.936947053	1.920870380
13	1.438897811	0.936947053	1.920870379
15	1.438897811	0.936947053	1.920870379
20	1.438897811	0.936947053	1.920870379
30	1.438897811	0.936947053	1.920870379
50	1.438897811	0.936947053	1.920870379

5. Numerical Scheme Testing

Here, we test the validity of our numerical results and contrast them with those of published works as limiting examples. So, we contrast the outcomes of this study with those found in references [8, 45, 49]. It is found that our results are in excellent agreement as shown in Table 2 and Table 3.

Table 2
Comparison of SLM finding of $-\theta'(0)$ and $-\phi'(0)$ with those found in Venkatesh *et al.,* [8] for various values of Nb when $Pr = 10, Le = 1, Nt = 0.3, M = 0.5, \beta_1 = 0.5, Du = Sr = \beta_2 = 0$

Nb	$-\theta'(0)$		$-\phi'(0)$	
	Venkatesh *et al.,* [8]	Present	Venkatesh *et al.,* [8]	Present
0.3	0.1352456	0.135273476	2.6031104	2.608854205
0.5	0.0836451	0.083719358	2.7463422	2.751788850
0.7	0.0570214	0.057153798	2.8405126	2.845554190

Table 3
Comparison of SLM finding of $f(\eta)$ with those found in Ghadikolaei *et al.,* [45] and Salah and Elhafian [49] for various values of η when $M = \beta_1 = \lambda = 0.0$ and $\beta_2 = 0.01$

β_2	η	Ghadikolaei *et al.,* [45]	Salah *et al.,* [49]	Present
	0	0	0	0
	0.1	0.095199	0.095194	0.095186
	0.2	0.181400	0.181338	0.181357
	0.5	0.394050	0.393892	0.393919
0.01	1	0.633463	0.633460	0.633440
	2	0.866679	0.867642	0.867634
	3	0.952228	0.954211	0.954216
	4	0.983566	0.986229	0.986225
	5	-	0.998059	0.998057

6. Results and Discussion

The successive linearization method was used to solve the boundary value issues numerically for the nonlinear-coupled ordinary differential Eq. (7) – (9) that are subject to the boundary conditions Eq. (10) – (12). The local skin-friction coefficient, the local Nusselt number, and the local Sherwood number are reported for various values of the physical parameters significant in this study based on the numerical computations are shown in Table 4.

Table 4
Different values of skin friction coefficient, local Nusselt number, and local Sherwood number using SLM for different parameters

M	Pr	Le	Nt	Nb	β_1	β_2	Du	Sr	$-f''(0)$	$-\theta'(0)$	$-\phi'(0)$
0.5	1	1	0.1	0.1	0.1	0.01	0.01	0.1	1.140131598	0.506098905	0.160887742
1.0									1.438897811	0.453772923	0.115316809
1.5									1.831538056	0.394398470	0.074358514
2.0									2.269832059	0.340515061	0.046535631
	1.0								1.438897811	0.453772923	0.115316809
	1.5								1.438897811	0.587002775	0.212434484
	2.0								1.438897811	0.687979451	0.314124511
	2.5								1.438897811	0.765978773	0.417662991
		1							1.438897811	0.453772923	0.115316809
		2							1.438897811	0.443471639	0.503256025
		3							1.438897811	0.438659866	0.795226329
		4							1.438897811	0.435838182	1.036453127
			0.1						1.438897811	0.453772923	0.115316809
			0.3						1.438897811	0.429680616	-0.510767431
			0.5						1.438897811	0.407114967	-1.065465848
			0.9						1.438897811	0.366232435	-1.990332651
				0.1					1.438897811	0.453772923	0.115316809
				0.3					1.438897811	0.411028304	0.360035767
				0.5					1.438897811	0.371053151	0.411116617
				0.9					1.438897811	0.299394175	0.448060675
					0.1				1.438897811	0.453772923	0.115316809
					0.5				1.557248634	0.423218683	0.091143214
					0.9				1.669815951	0.397070053	0.073515446
					1.2				1.750529310	0.379968549	0.063387989
						0.00			1.444537493	0.452917748	0.114614125
						0.02			1.433316189	0.454625073	0.116019001
						0.04			1.422319851	0.456320463	0.117421892
						0.06			1.411534832	0.458004227	0.118822767
							0.01		1.438897811	0.453772923	0.115316809
							0.05		1.438897811	0.441182734	0.126280363
							0.10		1.438897811	0.426450749	0.139074547
							0.20		1.438897811	0.399899039	0.162039380
								0.1	1.438897811	0.453772923	0.115316809
								0.3	1.438897811	0.455744046	0.044320247
								0.5	1.438897811	0.457724419	-0.027403698
								0.7	1.438897811	0.459714074	-0.099860882

Figure 2 shows that as the magnetic parameter M is increased, the fluid velocity decreases. A resistive force is produced in the direction of fluid flow as a result of the ongoing magnetic field. This resistive strength may reduce the momentum boundary layer's weight. As seen in Figure 3, decreasing velocity is the effect of increasing the elasticity parameter β_1. Physically speaking, it is known that

increasing the elastic parameter enhances the fluid stream's retardation, which causes the fluid velocity to decrease as the elastic parameter rises.

The impact of the Prandtl number Pr on fluid temperature is shown in Figure 4. The relative significance of the momentum boundary layer to the thermal boundary layer in the transport of heat is determined by the fluid's Prandtl number Pr. The fluid's temperature gradient reduces as Pr value rises. The momentum diffusivity rises and overtakes the thermal diffusivity as Pr rises.

The fluid's velocity is high enough to make a difference in the fluid's ability to transfer heat. As a result, the boundary layer becomes thinner, and the rate of heat dissipation increases.
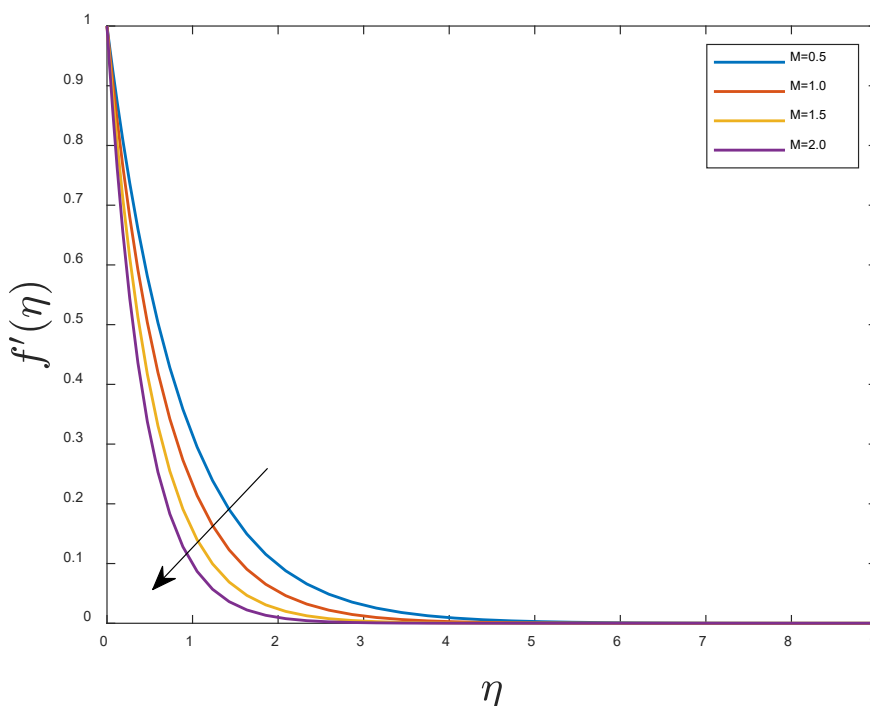
Fig. 2. Effect of M on velocity profile
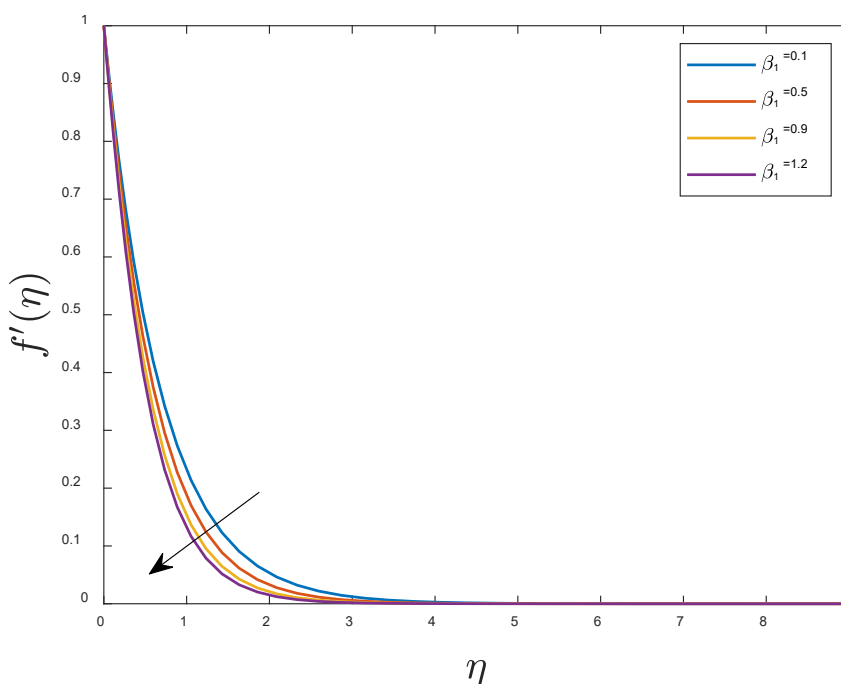
Fig. 3. Effect of β_1 on velocity profile
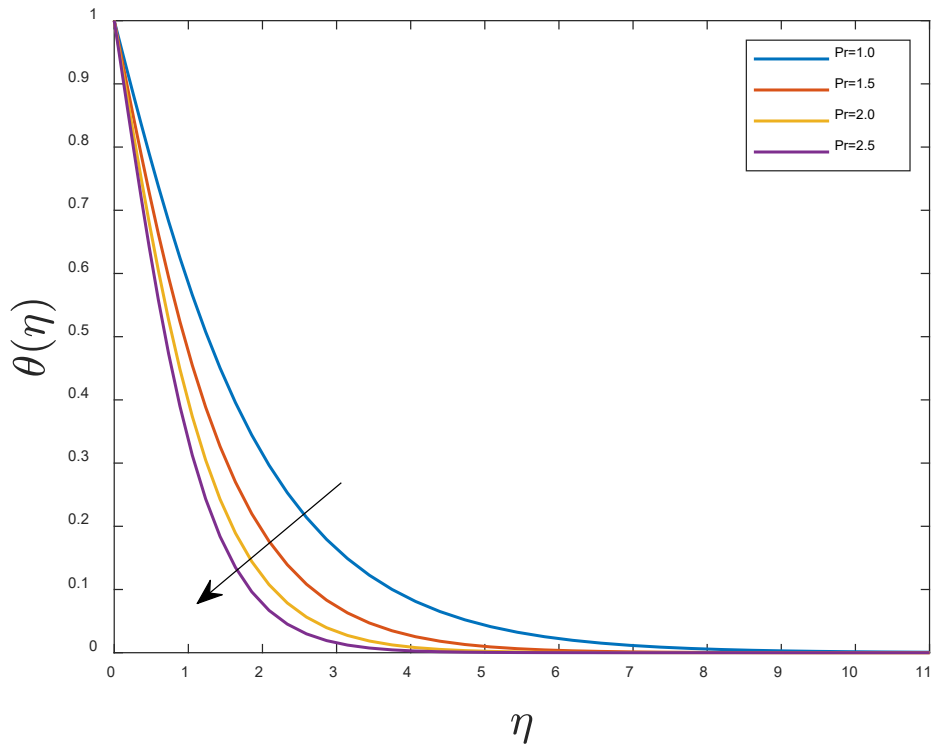
Fig. 4. Effect of Pr on temperature profile

Figure 5 illustrates the relationship between the temperature and the Dufour number Du. A concentration gradient causes a type of heat flow known as the Dufour effect. When the Dufour effect occurs, the temperature profiles are wider than when it does not. As the thermal boundary layer grows, boundary layer flow becomes electrified, and the Dufour number increases. Since the concentration gradient increases with an intensification of the Dufour factor, mass diffusion can occur more quickly as a result. Because of this, the temperature profile improves. Figure 6 illustrates the thermal boundary layer's temperature dispersion for various Brownian motion Nb values. A fluid's particles move randomly and erratically as a result of continuous collisions with other molecules. Temperature rises as a result of the kinetic energy of the fluid molecules being converted into thermal energy through the random movement of the nanoparticle when it collides with the molecules.

Figure 7 illustrates the temperature dispersion of the thermal boundary layer for different thermophoresis parameter values Nt. When there is a temperature differential, a transport force called thermophoresis results. The temperature improves as the amount of Nt rises because the boundary layer becomes heavier and heavier as it gets heavier. This happens because the surface temperature rises as a result.

Figure 8 depicts Le effects on concentration. The correlation between thermal diffusivity and mass diffusivity is referred to as the Lewis number. When there is simultaneous heat and mass transmission, it is utilized to describe fluid fluxes. As a result, the thickness of the thermal and concentration boundary layers is measured by the Lewis number. The Brownian diffusion coefficient has a major impact on the Lewis number Le. Higher Lewis number values help to reduce the Brownian diffusion coefficient, which reflects a lower concentration of nanoparticles.
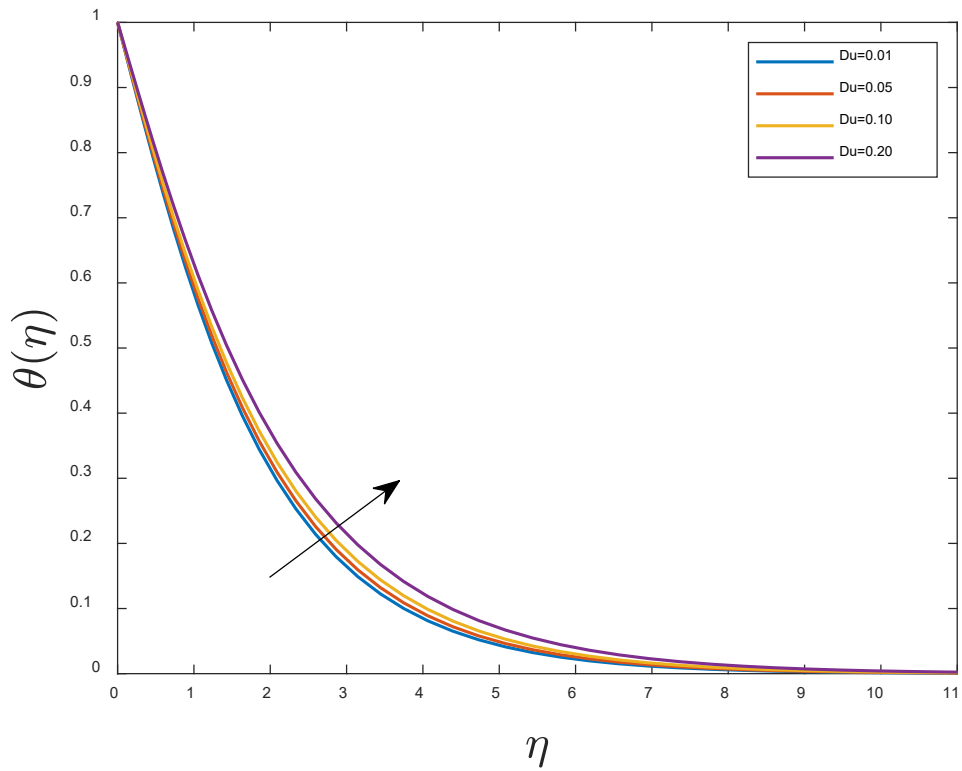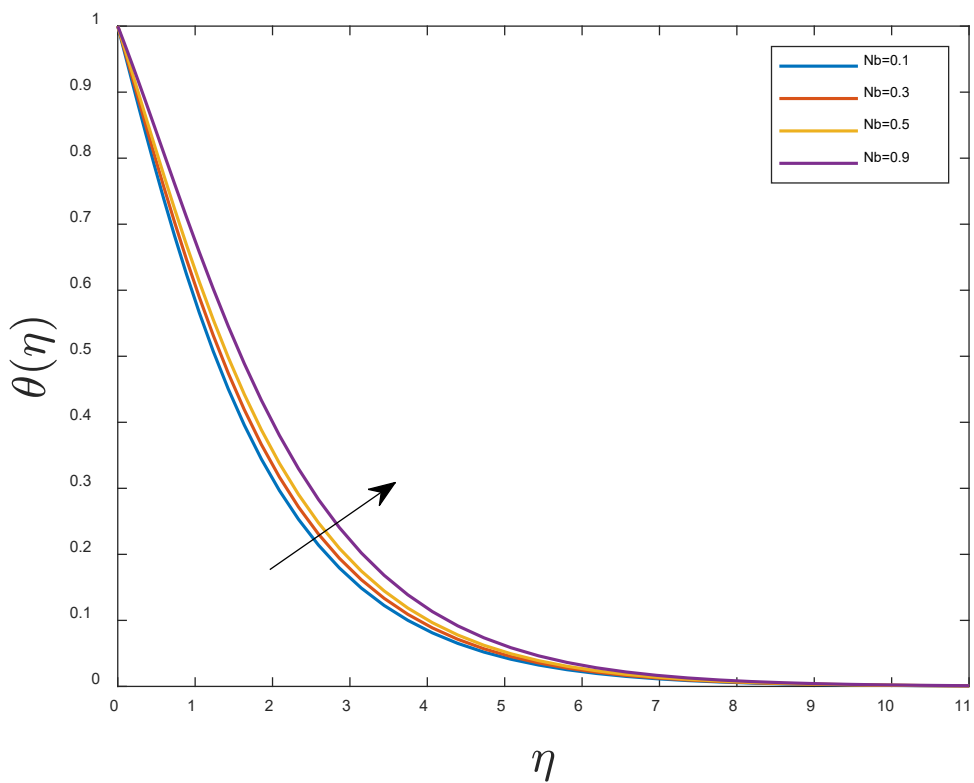
Fig. 5. Effect of Du on temperature profile

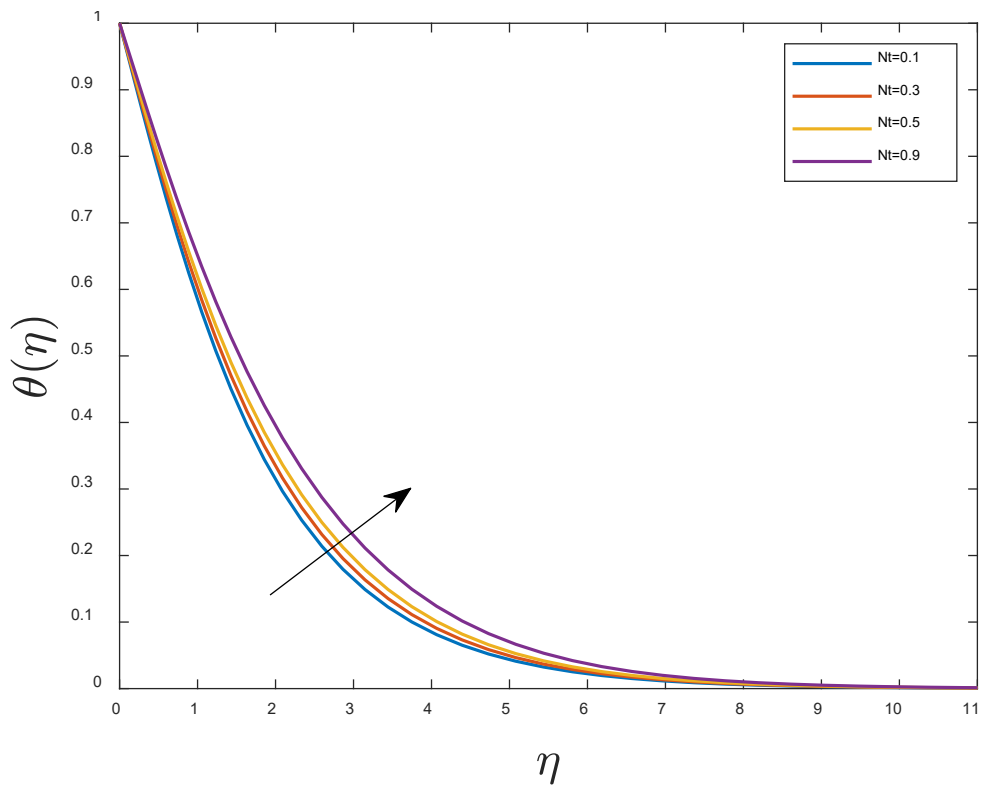**Fig. 6.** Effect of Nb on temperature profile

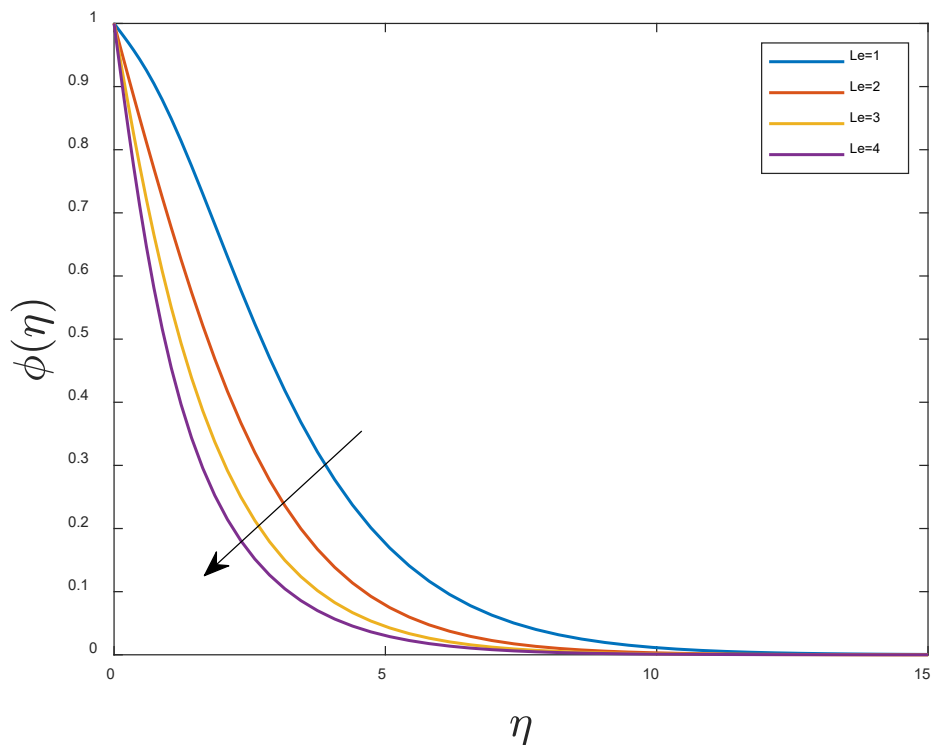**Fig. 7.** Effect of Nt on temperature profile

Fig. 8. Effect of Le on concentration profile

Figure 9 depicts the increasing nature of the concentration for various estimations of the Soret number Sr. The thermal diffusion (Soret) effect is the term used to describe the mass flux caused by a temperature gradient. It is plausible to infer that as the Soret effect has grown, so has the molar mass's diffusivity, raising the concentration. The Soret effect has enabled isotope separation and gas mixes with low molecular weights.

Finally, Figure 10 illustrate how β_2 affects the velocity profile. It should be noted that as β_2 is increased, the influence is found to be extremely minimal. Additionally, by setting $\beta_1 = 0$, $\beta_2 = 0$, and $\beta_1 = \beta_2 = 0$, the second-grade, Maxwell, and viscous cases are recovered respectively.
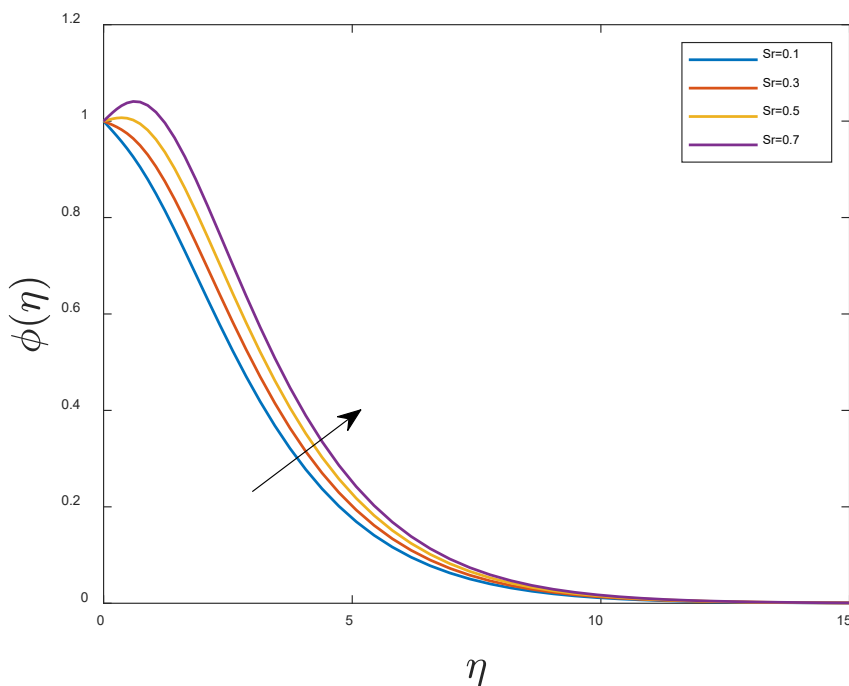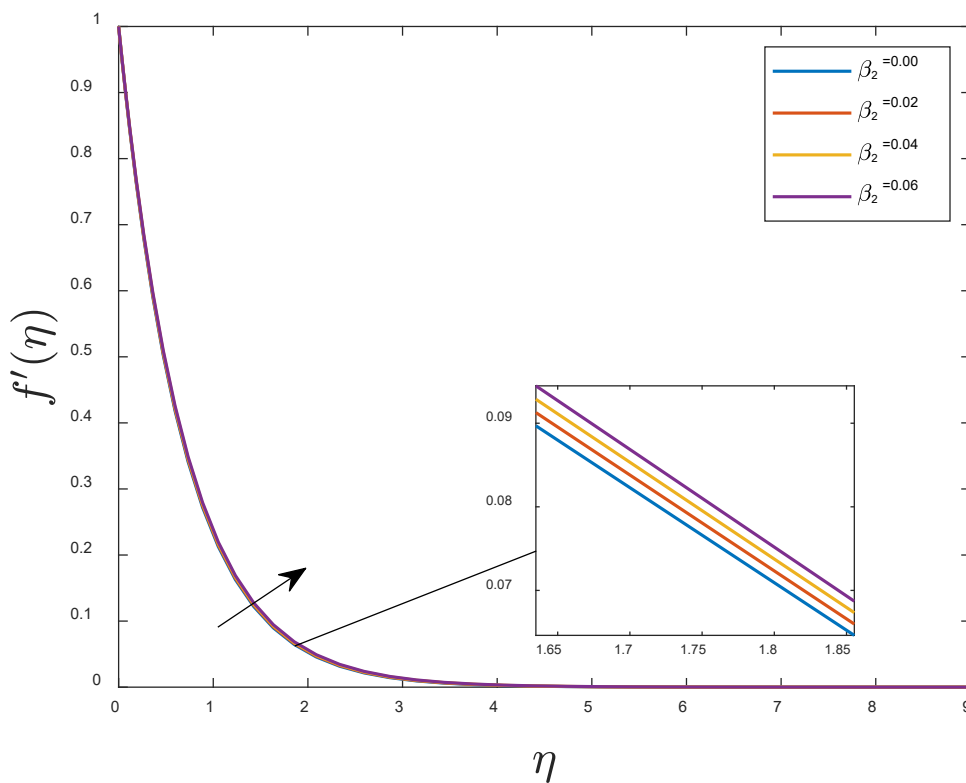

Fig. 9. Effect of Sr on concentration profile

Fig. 10. Effect of β_2 on velocity profile

7. Conclusions

In this study, we have discussed the heat and mass transfer characteristics of a two-dimensional incompressible Oldroyd-B fluid over a stretching sheet in the presence of Soret, Dufour, and nanoparticles. This fundamental issue arises in a variety of real-world contexts, including chemical engineering, geosciences, and the polymer extrusion process. The impact of the governing parameters, such as the magnetic parameter (M), elastic parameter (K), thermophoresis parameter (Nt), Brownian motion parameter (Nb), Lewis number (Le), and Prandtl number (Pr), on the velocity, temperature, and concentration profiles is discussed visually. These are the conclusions:

i.   The temperature and concentration distribution will improve as the Du and Sr levels rise.
ii. The velocity will decrease with rising β_1 and M values.
iii. Temperature profiles will climb with rising Pr values.
iv. Nusselt number estimates fall as Nb estimations rise.
v.   When Nb estimations rise, Sherwood estimates rise as well.
vi. The concentration profiles are getting flatter as Le values increase.

References

[1]   Hayat, Tasawar, Taseer Muhammad, Sabir Ali Shehzad, and Ahmed Alsaedi. "Temperature and concentration stratification effects in mixed convection flow of an Oldroyd-B fluid with thermal radiation and chemical reaction." *PloS one* 10, no. 6 (2015): e0127646. https://doi.org/10.1371/journal.pone.0127646

[2]   Khan, Ansab Azam, Khairy Zaimi, Suliadi Firdaus Sufahani, and Mohammad Ferdows. "MHD flow and heat transfer of double stratified micropolar fluid over a vertical permeable shrinking/stretching sheet with chemical reaction and heat source." *Journal of Advanced Research in Applied Sciences and Engineering Technology* 21, no. 1 (2020): 1-14. https://doi.org/10.37934/araset.21.1.114

[3]   Mahat, Rahimah, Muhammad Saqib, Imran Ulah, Sharidan Shafie, and Sharena Mohamad Isa. "MHD Mixed Convection of Viscoelastic Nanofluid Flow due to Constant Heat Flux." *Journal of Advanced Research in Numerical Heat Transfer* 9, no. 1 (2022): 19-25.

[4]   Hayat, T., Sohail A. Khan, A. Alsaedi, and Habib M. Fardoun. "Heat transportation in electro-magnetohydrodynamic flow of Darcy-Forchheimer viscous fluid with irreversibility analysis." *Physica Scripta* 95, no. 10 (2020): 105214. https://doi.org/10.1088/1402-4896/abb7aa

[5]   Shaqfeh, Eric SG. "Purely elastic instabilities in viscometric flows." *Annual Review of Fluid Mechanics* 28, no. 1 (1996): 129-185. https://doi.org/10.1146/annurev.fl.28.010196.001021

[6]   Laso, Manuel, and Hans Christian Öttinger. "Calculation of viscoelastic flow using molecular models: the CONNFFESSIT approach." *Journal of Non-Newtonian Fluid Mechanics* 47 (1993): 1-20. https://doi.org/10.1016/0377-0257(93)80042-a

[7]   Sajid, M., Z. Abbas, T. Javed, and N. Ali. "Boundary layer flow of an Oldroyd-B fluid in the region of a stagnation point over a stretching sheet." *Canadian Journal of Physics* 88, no. 9 (2010): 635-640. https://doi.org/10.1139/p10-049

[8]   Venkatesh, Nuka, Mella Anil Kumar, and Rallabandi Srinivasa Raju. "Dufour and Soret influence on MHD boundary layer flow of a Maxwell fluid over a stretching sheet with nanoparticles." *Heat Transfer* 51, no. 6 (2022): 5193-5205. https://doi.org/10.1002/htj.22543

[9]   Motsa, S. S., Z. G. Makukula, and S. Shateyi. "Numerical investigation of the effect of unsteadiness on three-dimensional flow of an Oldroyb-B fluid." *PLoS One* 10, no. 7 (2015): e0133507. https://doi.org/10.1371/journal.pone.0133507

[10] Hayat, Tasawar, Maria Imtiaz, Ahmed Alsaedi, and Saleh Almezal. "On Cattaneo–Christov heat flux in MHD flow of Oldroyd-B fluid with homogeneous–heterogeneous reactions." *Journal of Magnetism and Magnetic Materials* 401 (2016): 296-303. https://doi.org/10.1016/j.jmmm.2015.10.039

[11] Rajagopal, K. R., and R. K. Bhatnagar. "Exact solutions for some simple flows of an Oldroyd-B fluid." *Acta Mechanica* 113, no. 1-4 (1995): 233-239. https://doi.org/10.1007/bf01212645

[12] Hayat, T., S. A. Shehzad, A. Alsaedi, and M. S. Alhothuali. "Three-dimensional flow of Oldroyd-B fluid over surface with convective boundary conditions." *Applied mathematics and Mechanics* 34, no. 4 (2013): 489-500. https://doi.org/10.1007/s10483-013-1685-9

[13]   Hayat, Tasawar, Sabir Ali Shehzad, Saleh Al-Mezel, and Ahmed Alsaedi. "Three-dimensional flow of an Oldroyd-B fluid over a bidirectional stretching surface with prescribed surface temperature and prescribed surface heat flux." *Journal of Hydrology and Hydromechanics* 62, no. 2 (2014): 117. https://doi.org/10.2478/johh-2014-0016

[14]   Mabood, Fazle, Gabriella Bognár, and Anum Shafiq. "Impact of heat generation/absorption of magnetohydrodynamics Oldroyd-B fluid impinging on an inclined stretching sheet with radiation." *Scientific Reports* 10, no. 1 (2020): 17688. https://doi.org/10.1038/s41598-020-74787-2

[15]   Shankaralingappa, Bheemasandra M., Ballajja C. Prasannakumara, Bijjanal J. Gireesha, and Ioannis E. Sarris. "The impact of Cattaneo–Christov double diffusion on Oldroyd-B Fluid flow over a stretching sheet with thermophoretic particle deposition and relaxation chemical reaction." *Inventions* 6, no. 4 (2021): 95. https://doi.org/10.3390/inventions6040095

[16]   Yasir, Muhammad, Awais Ahmed, Masood Khan, Abdullah Khamis Alzahrani, Zaka Ullah Malik, and Ahmed Mohammad Alshehri. "Mathematical modelling of unsteady Oldroyd-B fluid flow due to stretchable cylindrical surface with energy transport." *Ain Shams Engineering Journal* 14, no. 1 (2023): 101825. https://doi.org/10.1016/j.asej.2022.101825

[17]   Liao, Shijun. *Beyond perturbation: introduction to the homotopy analysis method*. CRC press, 2003.

[18]   Makinde, O. D. "Effect of arbitrary magnetic Reynolds number on MHD flows in convergent-divergent channels." *International Journal of Numerical Methods for Heat & Fluid Flow* 18, no. 6 (2008): 697-707. https://doi.org/10.1108/09615530810885524

[19]   Makukula, Z., S. S. Motsa, and P. Sibanda. "On a new solution for the viscoelastic squeezing flow between two parallel plates." *Journal of Advanced Research in Applied Mathematics* 2, no. 4 (2010): 31-38. https://doi.org/10.5373/jaram.455.060310

[20]   Makukula, Zodwa G., Precious Sibanda, and Sandile S. Motsa. "A novel numerical technique for two-dimensional laminar flow between two moving porous walls." *Mathematical problems in Engineering* 2010 (2010). https://doi.org/10.1155/2010/528956

[21]   Narayana, Mahesha, and Precious Sibanda. "On the solution of double-diffusive convective flow due to a cone by a linearization method." *Journal of Applied Mathematics* 2012 (2012). https://doi.org/10.1155/2012/587357

[22]   Shateyi, S., and S. S. Motsa. "Variable viscosity on magnetohydrodynamic fluid flow and heat transfer over an unsteady stretching surface with Hall effect." *Boundary Value Problems* 2010 (2010): 1-20. https://doi.org/10.1155/2010/257568

[23]   Ahmed, Mohammed A. Mohammed, Mohammed E. Mohammed, and Ahmed A. Khidir. "On linearization method to MHD boundary layer convective heat transfer with low pressure gradient." *Propulsion and Power Research* 4, no. 2 (2015): 105-113. https://doi.org/10.1016/j.jppr.2015.04.001

[24]   Khidir, Ahmed A. "Application of Successive Linearisation Method on Mixed Convection Boundary Layer Flow of Nanofluid from an Exponentially Stretching Surface with Magnetic Field Effect." *Journal of Nanofluids* 12, no. 2 (2023): 465-475. https://doi.org/10.1166/jon.2023.1961

[25]   Daoud, Yassir, Mohammed Abdalbagi, and Ahmed A. Khidir. "On the solution of magneto-hydrodynamics three-dimensional flow due to a stretching sheet in a porous medium using the successive linearization method." *Chinese Journal of Physics* 73 (2021): 232-238. https://doi.org/10.1016/j.cjph.2021.06.011

[26]   Salah, F., Alzahrani, A. K., Sidahmed, A. O., & Viswanathan, K. K. "A note on thin-film flow of Eyring-Powell fluid on the vertically moving belt using successive linearization method." *International Journal of Advanced and Applied Sciences* 6.2 (2019): 17-22. https://doi.org/10.21833/ijaas.2019.02.004

[27]   Venkateswarlu, B., and PV Satya Narayana. "Soret and Dufour effects on MHD flow of a Maxwell fluid over s stretching sheet with joule heating." *Front Heat Mass Trans* 8 (2017): 1-5. https://doi.org/10.5098/hmt.9.11

[28]   Hayat, T., S. A. Shehzad, and A. Alsaedi. "Soret and Dufour effects on magnetohydrodynamic (MHD) flow of Casson fluid." *Applied Mathematics and Mechanics* 33 (2012): 1301-1312. https://doi.org/10.1007/s10483-012-1623-6

[29]   Khan, Sohail A., T. Hayat, and A. Alsaedi. "Simultaneous features of Soret and Dufour in entropy optimized flow of Reiner-Rivlin fluid considering thermal radiation." *International Communications in Heat and Mass Transfer* 137 (2022): 106297. https://doi.org/10.1016/j.icheatmasstransfer.2022.106297

[30]   Khan, Sohail A., T. Hayat, and A. Alsaedi. "Numerical study for entropy optimized radiative unsteady flow of Prandtl liquid." *Fuel* 319 (2022): 123601. https://doi.org/10.1016/j.fuel.2022.123601

[31]   Jawad, Muhammad, Anwar Saeed, Arshad Khan, Ishtiaq Ali, Hussam Alrabaiah, Taza Gul, Ebenezer Bonyah, and Muhammad Zubair. "Analytical study of MHD mixed convection flow for Maxwell nanofluid with variable thermal conductivity and Soret and Dufour effects." *AIP Advances* 11, no. 3 (2021). https://doi.org/10.1063/5.0029105

[32]   Reddy, M. Vinodkumar, Lakshminarayana Pallavarapu, and Kuppalapalle Vajravelu. "Magnetohydrodynamic radiative flow of a Maxwell fluid on an expanding surface with the effects of Dufour and Soret and chemical reaction." *Computational Thermal Sciences: An International Journal* 12, no. 4 (2020). https://doi.org/10.1615/computthermalscien.2020034147

[33] Hosseinzadeh, Kh, M. R. Mardani, Sajad Salehi, M. Paikar, M. Waqas, and D. D. Ganji. "Entropy generation of three-dimensional Bödewadt flow of water and hexanol base fluid suspended by Fe _ 3 O _ 4 Fe 3 O 4 and MoS _ 2 MoS 2 hybrid nanoparticles." *Pramana* 95 (2021): 1-14. https://doi.org/10.1007/s12043-020-02075-9

[34] Gholinia, M., SAH Kiaeian Moosavi, M. Pourfallah, S. Gholinia, and D. D. Ganji. "A numerical treatment of the TiO2/C2H6O2–H2O hybrid base nanofluid inside a porous cavity under the impact of shape factor in MHD flow." *International Journal of Ambient Energy* 42, no. 16 (2021): 1815-1822. https://doi.org/10.1080/01430750.2019.1614996

[35] Doh, Deog-Hee, M. Muthtamilselvan, B. Swathene, and E. Ramya. "Homogeneous and heterogeneous reactions in a nanofluid flow due to a rotating disk of variable thickness using HAM." *Mathematics and Computers in Simulation* 168 (2020): 90-110. https://doi.org/10.1016/j.matcom.2019.08.005

[36] Dadheech, P. K., P. Agrawal, F. Mebarek-Oudina, N. H. Abu-Hamdeh, and A. Sharma. "Comparative heat transfer analysis of MoS2/C2H6O2 and SiO2-MoS2/C2H6O2 nanofluids with natural convection and inclined magnetic field." *Journal of Nanofluids* 9, no. 3 (2020): 161-167. https://doi.org/10.1166/jon.2020.1741

[37] Marzougui, Souad, Fateh Mebarek-Oudina, Mourad Magherbi, and Ali Mchirgui. "Entropy generation and heat transport of Cu–water nanoliquid in porous lid-driven cavity through magnetic field." *International Journal of Numerical Methods for Heat & Fluid Flow* 32, no. 6 (2021): 2047-2069. https://doi.org/10.1108/hff-04-2021-0288

[38] Chabani, Ines, Fateh Mebarek-Oudina, and Abdel Aziz I. Ismail. "MHD flow of a hybrid nano-fluid in a triangular enclosure with zigzags and an elliptic obstacle." *Micromachines* 13, no. 2 (2022): 224. https://doi.org/10.3390/mi13020224

[39] Wang, Fuzhang, M. Waqas, W. A. Khan, Basim M. Makhdoum, and Sayed M. Eldin. "Cattaneo–Christov heat-mass transfer rheology in third-grade nanoliquid flow confined by stretchable surface subjected to mixed convection." *Computational Particle Mechanics* (2023): 1-13. https://doi.org/10.1007/s40571-023-00579-w

[40] Pasha, Amjad Ali, Zubair Hussain, Md Mottahir Alam, Navin Kasim, Kashif Irshad, Mehboob Ali, Muhammad Waqas, and Waqar Azeem Khan. "Impact of magnetized non-linear radiative flow on 3D chemically reactive sutterby nanofluid capturing heat sink/source aspects." *Case Studies in Thermal Engineering* 41 (2023): 102610. https://doi.org/10.1016/j.csite.2022.102610

[41] Nasir, M., M. Waqas, O. A. Bég, H. F. M. Ameen, N. Zamri, K. Guedri, and S. M. Eldin. "Analysis of Nonlinear Convection–Radiation in Chemically Reactive Oldroyd-B Nanoliquid Configured by a Stretching Surface with Robin Conditions: Applications in Nano-Coating Manufacturing. Micromachines 2022, 13, 2196." (2022). https://doi.org/10.3390/mi13122196

[42] Tabrez, Muhammad, Waqar Azeem Khan, Taseer Muhammad, Iftikhar Hussain, and Muhammad Waqas. "Significance of thermo-dynamical moment of ferromagnetic nanoparticles and bioconvection analysis for magnetized Carreau fluid under the influence of gyrotactic moment of microorganisms." *Tribology International* 186 (2023): 108633. https://doi.org/10.1016/j.triboint.2023.108633

[43] Cortell, Rafael. "A note on flow and heat transfer of a viscoelastic fluid over a stretching sheet." *International Journal of Non-Linear Mechanics* 41.1 (2006): 78-85.

[44] Salah F. "Numerical solution for heat transfer of Oldroyd-B fluid over a stretching sheet using successive linearization method." *International Journal of Advance and Applied Science*, 7.6 (2020): 40-47. https://doi.org/10.21833/ijaas.2020.06.006

[45] Ghadikolaei, S. S., Kh Hosseinzadeh, M. Yassari, H. Sadeghi, and D. D. Ganji. "Analytical and numerical solution of non-Newtonian second-grade fluid flow on a stretching sheet." *Thermal Science and Engineering Progress* 5 (2018): 309-316. https://doi.org/10.1016/j.tsep.2017.12.010

[46] Makukula, ZodwaG, Precious Sibanda, and SandileSydney Motsa. "A note on the solution of the von Kármán equations using series and Chebyshev spectral methods." *Boundary Value Problems* 2010 (2010): 1-17. https://doi.org/10.1155/2010/471793

[47] Ahmed, Mohammed A. Mohammed, Mohammed E. Mohammed, and Ahmed A. Khidir. "The effects of cross-diffusion and radiation on mixed convection from a vertical flat plate embedded in a fluid-saturated porous medium in the presence of viscous dissipation." *Propulsion and Power Research* 5, no. 2 (2016): 149-163. https://doi.org/10.1016/j.jppr.2016.05.001

[48] Sidahmed, Abdelmgid, and Faisal Salah. "Radiation effects on MHD flow of second grade fluid through porous medium past an exponentially stretching sheet with chemical reaction." *Journal of Advanced Research in Fluid Mechanics and Thermal Sciences* 99, no. 2 (2022): 1-16. https://doi.org/10.37934/arfmts.99.2.116

[49] Salah, Faisal, and Mubarak H. Elhafian. "Numerical Solution for Heat Transfer of Non-Newtonian Second-Grade Fluid Flow over Stretching Sheet via Successive Linearization Method." *IAENG International Journal of Applied Mathematics* 49, no. 4 (2019).

[50] Hussaini, M. Y., & Zang, T. A. "Spectral methods in fluid dynamics." *Annual review of fluid mechanics*, *19*.1, (1987): 339-367.